A methodology to estimate average flow rates in Water Supply Systems (WSSs) for energy recovery purposes through hydropower solutions

A methodology to estimate average flow rates in Water Supply Systems (WSSs) for energy recovery purposes through hydropower solutions

Mosè Rossi[a], Samuele Spedaletti[a,b], Matteo Lorenzetti[b], Danilo Salvi[b], Massimiliano Renzi[c], Gabriele Comodi[a,*], Flavio Caresana[a], Leonardo Pelagalli[a]

[a] Marche Polytechnic University, Department of Industrial Engineering and Mathematical Sciences, Via Brecce Bianche 12, Ancona – 60131, Italy

[b] Astea S.p.A., Via Guazzatore 163, Osimo (AN) – 60027, Italy

[c] Free University of Bozen-Bolzano, Faculty of Science and Technology, Piazza Università 1, Bolzano – 39100, Italy

*Corresponding author: Gabriele Comodi, PhD, Associate Professor. Faculty of Engineering, Department of Industrial Engineering and Mathematical Sciences, Marche Polytechnic University, Via Brecce Bianche 12, 60131, Ancona, Italy. E-mail: g.comodi@univpm.it.

ABSTRACT

Energy efficiency interventions in Water Supply Systems (WSSs) need a precise evaluation of the available water flow rates for energy recovery interventions; however, flow meters are generally too costly for being installed in all the gravity adduction pipelines of a WSS. This paper presents a methodology for predicting flow rates in gravity adduction pipelines based on the electricity bill consumption. In this study, the predicted average flow rate is 0.0300 $m^3 * s^{-1}$, being 1.64% lower than the real one. A Pelton turbine has been chosen as energy recovery unit for supplying electricity to a pumping station of a preloading tank where the water is treated to make it drinkable. An energy saving of 475.26 (MW*h)*$year^{-1}$ is achieved, which can be also expressed as 88.87 saved Tonnes of Oil Equivalent (TOE) and 204.36 $ktCO_2$ not released into the atmosphere. The gross economic saving due to the installation of the Pelton turbine is equal to 94.29 k€*$year^{-1}$ and it can be further increased

up to 116.51 k€*year^{-1} if the energy efficiency certificates issued by the Italian Authorities are considered. The Payback Period (PBP) of the intervention corresponds to 3 years, and a Net Present Value (NPV) after twenty years is approximately 1.4 M€.

KEYWORDS

Economic saving; Energy efficiency; Flow rate estimation; Pelton turbine; Small-scale hydropower; Water Supply System.

NOMENCLATURE

$\mathrm{A_{ind}}$ = Area occupied by industrial users [m^2]

$\mathrm{A_{res}}$ = Area occupied by residential users [m^2]

$\mathrm{Ec_{eec}}$ = Economic saving due to the energy efficiency certificates [€*year^{-1}]

$\mathrm{Ec_{saving\_gross}}$ = Gross economic saving [€*year^{-1}]

$\mathrm{Ec_{saving\_gross\_final}}$ = Gross economic saving considering the energy efficiency certificates [€*year^{-1}]

$\overline{\mathrm{En}}_{\mathrm{after\_turbine}}$ = Electric energy consumed by the pumping station after the installation of the hydraulic turbine [MW*h]

$\overline{\mathrm{En}}_{\mathrm{before\_turbine}}$ = Electric energy consumed by the pumping station before the installation of the hydraulic turbine [MW*h]

$\overline{\mathrm{En}}_{\mathrm{electric\_bill}}$ = Average electricity bill consumption of the pumping station [MW*h]

$\overline{\mathrm{En}}_{\mathrm{electric\_pump}}$ = Average electricity consumption of the pumping station [MW*h]

$\overline{\mathrm{En}}_{\mathrm{electric\_pump,i}}$ = Average electricity consumption of a hydraulic pump [MW*h]

$\overline{\text{En}}_{\text{electric\_turbine avg\_monthly}}$ = Monthly average electric energy produced by the hydraulic turbine [MW*h]

$\overline{\text{En}}_{\text{saving\_after\_turbine}}$ = Electric energy saving after the installation of the hydraulic turbine [MW*h]

Fc_{tCO2} = Conversion factor from kW*h to tCO_2 [tCO_2*(kW*h)$^{-1}$]

Fc_{TOE} = Conversion factor from kW*h to TOE [TOE*(kW*h)$^{-1}$]

F_{ec} = Conversion factor from kW*h to € [€*(kW*h)$^{-1}$]

F_{eec} = Conversion factor from TOE to € [€*TOE^{-1}]

g = Gravity acceleration [m*s^{-2}]

H = Head [m]

$H_{available}$ = Available head [m]

H_{loss} = Head losses [m]

H_{useful} = Useful head [m]

n_{ind} = Population density in industrial areas [person*m^{-2}]

n_{res} = Population density in residential areas [person*m^{-2}]

$\overline{P}_{\text{hydraulic avg\_yearly}}$ = Average available hydraulic power [kW]

$\overline{P}_{\text{turbine avg\_monthly}}$ = Average power produced by the hydraulic turbine [kW]

$\dot{Q}$ = Flow rate [m^3*s^{-1}]

$\overline{\dot{Q}}_{\text{avg\_yearly}}$ = Yearly average flow rate in a gravity adduction pipeline [m^3*s^{-1}]

$\overline{\dot{Q}}_{\text{pump avg\_monthly}}$ = Monthly average flow rate elaborated by the pumping station [m^3*s^{-1}]

$\bar{\dot{Q}}_{pump,i\ avg\_monthly}$ = Monthly average flow rate elaborated by a hydraulic pump [m^3*s^{-1}]

$\bar{\dot{Q}}_{turbine\ avg\_monthly}$ = Measured monthly average flow rate elaborated by the hydraulic turbine [m^3*s^{-1}]

$\bar{\dot{Q}}_{turbine\ avg\_monthly\_meas}$ = Measured yearly average flow rate elaborated by the hydraulic turbine [m^3*s^{-1}]

$\bar{\dot{Q}}_{turbine\ avg\_monthly\_model}$ = Estimated monthly average flow rate potentially elaborated by the hydraulic turbine [m^3*s^{-1}]

$\bar{\dot{Q}}_{turbine\ avg\_yearly}$ = Measured average flow rate elaborated by the hydraulic turbine [m^3*s^{-1}]

$\bar{\dot{Q}}_{turbine\ avg\_yearly\_model}$ = Estimated yearly average flow rate potentially elaborated by the hydraulic turbine [m^3*s^{-1}]

$\bar{\dot{Q}}_{wells\ avg\_monthly}$ = Monthly average flow rate coming from the wells [m^3*s^{-1}]

$V_{monthly,end\ user,i}$ = Monthly water volume consumption of a generic end user [m^3]

$V_{monthly\_ind}$ = Monthly water volume consumption per each residential user [m^3]

$V_{monthly\_res}$ = Monthly water volume consumption per each industrial user [m^3]

$\mathbf{tCO_{2\_saving}}$ = Tonnes of CO_2 [tCO_2] saving

TOE_{saving} = Tonnes of Oil Equivalent [TOE] saving

$\Delta\bar{\dot{Q}}$ = Relative percentage error related to the flow rate estimation [%]

η_{pump} = Total efficiency of a hydraulic pump [-]

$\eta_{turbine}$ = Total efficiency of the hydraulic turbine [-]

ρ = Water density at normal conditions [kg*m^{-3}]

ω = Angular rotational speed [rad*s^{-1}]

ω_s = Specific rotational speed [-]

ACRONYMS

BEP = Best Efficiency Point

NPV = Net Present Value

O&M = Operation & Management

PBP = Payback Period

PID = Proportional-Integral-Derivative

PRV = Pressure Reducing Valve

PSO = Particle Swarm Optimization

TOE = Tonnes of Oil Equivalent

WDN = Water Distribution Network

WSS = Water Supply System

1. INTRODUCTION

The water-energy nexus concept is becoming of great interest in the energy sector with the aim of ensuring a sustainable exploitation of the water source on both environmental and energy points of view [1, 2]. Within the water-energy nexus framework, one of the most important topics concerns the use of water for power production. Hydropower plants generate clean energy by exploiting the energy potential of a water reservoir and transforming it to electricity by a generator. Conversely, a considerable amount of energy is required by several processes to pump and treat water in civil and industrial contexts. The two perspectives can be combined in several applications, like in Water Supply Systems (WSSs), Water Distribution Networks (WDNs) [3, 4] and in wastewater treatment plants [5, 6] where a share of the energy required to run such plants can be potentially recovered. All the previous mentioned applications present facilities, such as the pumping stations, that are highly energy consuming, but also with considerable hydraulic head potentials. For this reason, the recovered energy can lead to an increase of the system efficiency, thus to a reduction of both consumed Tonnes of Oil Equivalent (TOE) and CO_2 emissions released into the atmosphere [7, 8].

WSSs are typically constituted by a water source connected to loading/head compensation tanks downstream located at high geodetic altitudes, being in turn connected to other tanks [9] or directly to the end users via distribution network. The extension of WSSs depends on the number of inhabitants of a city/town, as well as on its dimensions. The water source can be a reservoir filled by water pumped from a low-level reservoir. About 2-3% of the electric energy consumption worldwide derives from pumping stations of WSSs [10, 11] and 80-90% of this consumption is addressed to pump motors [12, 13]. In this regard, some works in literature stated that the specific energy consumptions measured in WSSs are below 0.30 $(kW*h)*m^{-3}$ in developing countries and reach values higher than 3 $(kW*h)*m^{-3}$ in developed ones [14, 15]; in this last case, energy recovery interventions are strongly recommended to improve the efficiency of WSSs.

The proper choice of the energy recovery intervention in WSSs depends on their design characteristics [16, 17] and several authors investigated on the energy recovery potential through hydropower solutions. Kucukali [18] estimated that this kind of recovery potential, which has been applied in 45 WSSs located in Turkey, led to 173 GW*h saved per year. McNabola et al. [19] analysed ten cases related to water industries in Ireland, where the hydraulic power is recovered through small-scale hydropower plants ranging between 2 and 115 kW. The installation of hydraulic turbines in WSSs provides, beside the electricity production, the water pressure regulation inside the network, which is usually performed by Pressure Reducing Valves (PRVs). Indeed, a reduction of the water pressure leads to a decrease of the water losses throughout the pipelines [20, 21] that reached nowadays a remarkable average value of 26% worldwide [22]. PRVs are installed not only in WDNs, but also in WSSs where high values of pressure are present. For instance, this situation occurs when an upstream water source is placed at a very high altitude and connected to a preloading or a loading/head compensation tank downstream that is at atmospheric pressure. The preloading tank has the aim to mix the water coming from the water source with the one coming from wells, whose chemical properties are not still acceptable. After the mixing process, the water becomes drinkable and it is pumped to loading/head compensation tanks; subsequently, it is distributed to the end users via distribution network. However, pumping stations withdraw water from the preloading tank and provide it with the proper pressure in order to reach loading/head compensation tanks. Doing this, the potential energy content of the water due to the geodetic altitude difference between the water source and the preloading tank is lost, since it is dissipated through a PRV for being lowered down to the atmospheric pressure. It is worth noting that the mixing process can be also performed inside the pipelines, unless the water pressure is enough to provide the water to loading/head compensation tanks.

In order to improve the efficiency of WSSs, hydraulic turbines can be installed upstream the preloading tank, thus replacing PRVs in order to recover part of this water energy content and produce the electric energy required by the pumping station. The installation of small-scale hydropower plants in WSSs presents low implementation costs [23, 24]. The produced electric energy can be consumed by facilities and auxiliary systems of WSSs, thus lowering the amount of electricity withdrawn by the national grid [18]. Energy recovery interventions through hydropower solutions in WSSs have also three main advantages [25]: i) reduction of the greenhouse gas emissions due to the self-consumption of the produced electric energy, as well as its production by means of a renewable source, ii) limitation of civil works since they are adapted to the existing infrastructure, thus not requiring new spaces, and iii) to lower environmental impacts throughout the life cycle of WSSs.

Nevertheless, the correct average flow rate in gravity adduction pipelines has to be assessed in order to perform the energy recovery interventions properly, mostly when flow meters are not installed. In literature there are several works, based on the evaluation of the water demand of the end users, that analysed different deterministic, probabilistic and demand time-series approaches for predicting the peak demand in WSSs. In this regard, Wong et al. [26] carried out a literature review on the previous mentioned approaches and proposed the Bayesian one, which bridges the gap between model-based and field-measurement values, being more flexible and more reliable on the design point of view. Letting et al. [27] presented a simulation model for the water demand using a Particle Swarm Optimization (PSO) algorithm and compared the numerical results with the real ones obtained by sensors. Results showed that both nodal demands and pipe flows can be accurately determined. Balacco et al. [28] analysed the water demand in several towns in Puglia (Italy), leading to the definition of a relationship between the peak factor and the number of inhabitants. They found out that the design of WSSs can be done without considering the use of monthly and weekly peak factors. Moreover, the magnitude of the peak factor obtained through measured data is considerably lower compared to the literature values. However, detailed information related to WSSs and WDNs are usually required, which are not always affordable and make difficult, as well as time demanding, the calculation of the water demand, also considering the creation of optimization algorithms. Moreover, to the authors' knowledge, a methodology to estimate the yearly average flow rate in gravity adduction pipelines has not be discussed and presented so far.

In this work, a methodology based on the knowledge of the electricity bill consumption related to the pumping station of a preloading tank to predict the yearly average flow rate that can be potentially exploited for energy recovery purposes is presented. In particular, this methodology is thought to be applied in branches where flow meters are not installed. First of all, gravity adduction pipelines where the hydraulic turbine can be installed have to be identified, taking into account the connections between a water source and the preloading tank. The developed methodology was then validated through measured data obtained by a flow meter installed upstream the preloading tank, after the hydraulic turbine installation. Finally, energy, environmental and economic analyses have been performed to assess the advantages of this energy efficiency intervention.

The present paper is structured as follows: Section 2 describes the methodology developed for estimating the yearly average flow rate when flow meters are not installed; then, the head that can be exploited by the hydraulic turbine has been also calculated using a formula reported in literature. In addition, the procedure to select the proper machine is also presented. Section 3 deals with the case study of a WSS related to a mid-town located in the Center of Italy. After the analysis of the flow duration curve of the site of interest, the flow rates obtained through the methodology described in Section 2 have been confirmed and validated with measured data from a flow meter installed after the hydraulic turbine installation, whose selection process has led to the choice of a Pelton machine. Section 4 presents energy, environmental and economic analyses due to the energy efficiency intervention. Finally, Section 5 reports the conclusions of the work.

2. METHODOLOGY

This Section aims at describing a methodology capable of identifying the hydropower potential in WSSs through the estimation of the flow rates in gravity adduction pipelines that connect the water source to the preloading tanks downstream. The presented methodology is based on the knowledge of the electricity bill consumption of the pumping station installed in the preloading tank. After the estimation of the yearly average flow rate, the head is evaluated by knowing the geodetic heights of each element previously mentioned in the site of interest and the relative head losses. The methodology is divided in three phases:

i) analysis of the WSS structure of the site of interest, taking into account the WSS layout composed by a water source, a preloading tank with a pumping station, loading/head compensation tanks and interconnections;
ii) estimation of the hydropower potential from sites identified in the previous phase, focusing the attention to the one having the connection between the water source and the preloading tank. Then, after the analysis of the flow duration curve, the yearly average flow rate, together with the useful head, are calculated. Finally, the calculation of the power produced by the hydropower system is also provided;
iii) assessment of energy, environmental and economic benefits due to the hydraulic turbine installation; specifically, the evaluation of the energy saving, also in terms of saved TOE and tCO_2 emissions not released into the atmosphere, and the economic saving due to the energy efficiency intervention are discussed.

2.1 Water Supply System (WSS) infrastructure and an overview of the site of interest

The water reservoir of the analysed WSS is located at 346 m a.s.l. with a height of 69.4 m (55 m of depth) and a capacity of 37.3 Mm^3. The water coming from this reservoir feeds one preloading tank and then seven loading tanks placed in different zones, as reported in Figure 1 and Table 1.

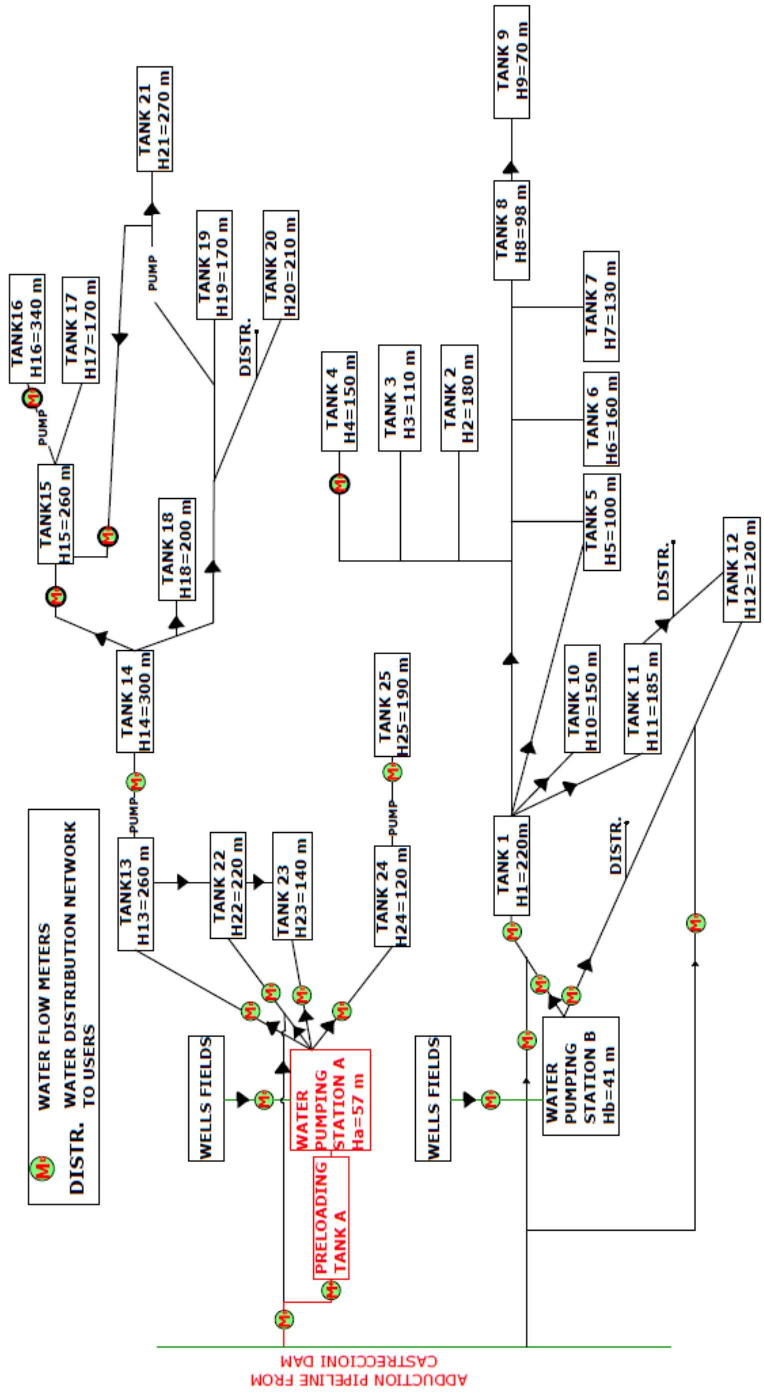

Figure 1: Layout of the analysed WSS

Table 1: Water source, loading, preloading and head compensation tanks with respective geodetic heights

WATER SOURCE	LOADING AND PRELOADING TANK (GEODETIC HEIGTH)	HEAD COMPENSATION TANK (GEODETIC HEIGTH)	GEODETIC HEIGTH DIFFERENCE
CASTRECCIONI DAM (346 m)	TANK A (57 m)	-	289 m
	-	TANK 1 (57 m)	126 m
	-	TANK 22 (220 m)	126 m
	-	TANK 12 (120 m)	226 m
	TANK 13 (260 m)	TANK 22 (220 m)	40 m
	TANK 22 (220 m)	TANK 23 (140 m)	80 m
	TANK 14 (300 m)	TANK 18 (200 m)	100 m
		TANK 19 (170 m)	130 m
		TANK 20 (210 m)	90 m
		TANK 15 (260 m)	40 m
	TANK 15 (260 m)	TANK 17 (170 m)	90 m
	TANK 1 (220 m)	TANK 2 (180 m)	40 m
		TANK 3 (110 m)	110 m
		TANK 4 (150 m)	70 m
		TANK 5 (100 m)	120 m
		TANK 6 (160 m)	60 m
		TANK 7 (130 m)	90 m
		TANK 8 (98 m)	122 m
		TANK 10 (150 m)	70 m
		TANK 11 (185 m)	35 m
	TANK 11 (185 m)	TANK 12 (120 m)	65 m
	TANK 8 (98 m)	TANK 9 (70 m)	28 m

In particular, Tank A is the preloading tank that collects the water coming from both water source and wells with the aim of making it drinkable after a mixing phase process. The preloading tank presents a pumping station that supplies water to Tanks 13, 22, 23 and 24 located at higher altitudes with respect to the preloading tank itself. Figure 2 shows a simplified scheme of the site of interest, namely the preloading tank where a hydraulic turbine has been subsequently installed.

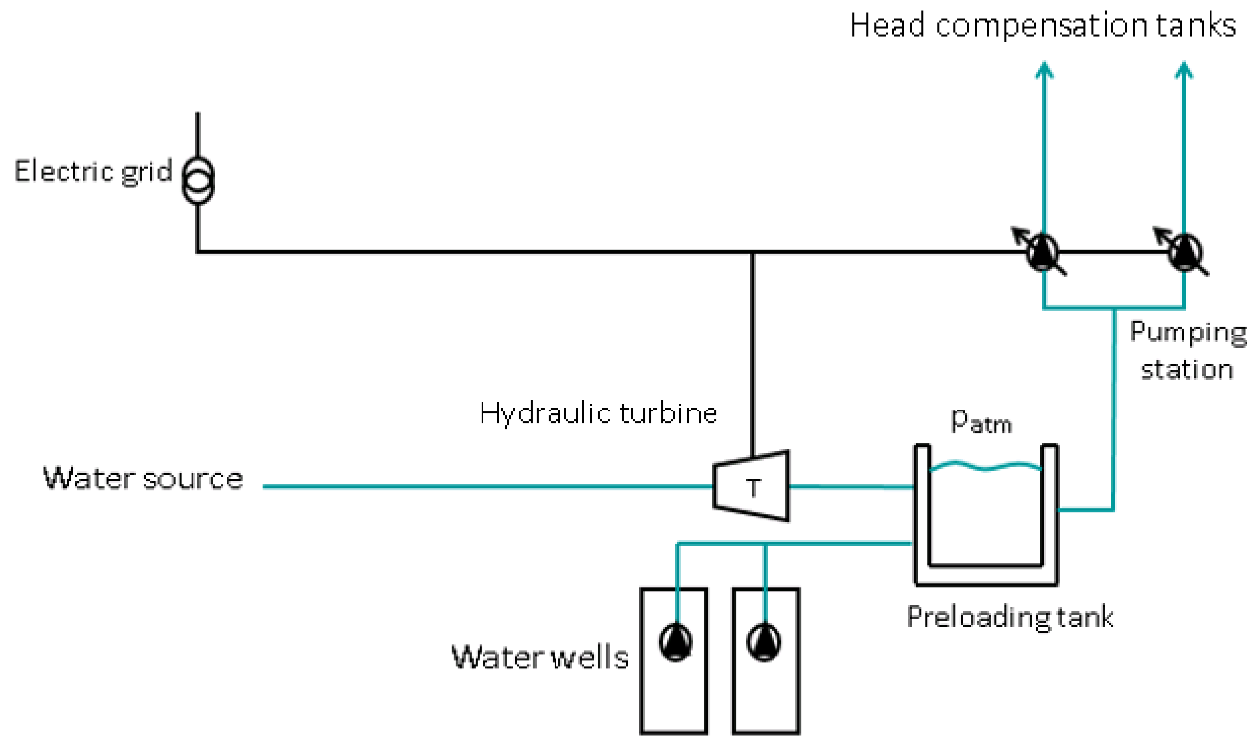

Figure 2: Simplified scheme of the site of interest (preloading tank plus the new hydraulic turbine)

2.2 Estimation of both yearly average flow rate and useful head of the hydraulic turbine

The flow rate elaborated by the hydraulic turbine can correspond either to the overall one that flows in gravity adduction pipelines or to a part of it, according to the number of deviations and design characteristics of the WSS. The evaluation of the flow rate can be done instrumentally through flow meters installed in pipelines that recreate the flow duration curve.

Generally, flow meters are installed in adduction pipelines that connect the pumping stations to a loading/head compensation tank located at high altitude, while it is rare to find them in gravity adduction pipelines since they are costly. If a gravity adduction pipeline connects the water source to a loading/head compensation tank directly, the yearly average flow rate $\bar{\dot{Q}}_{\text{avg\_yearly}}$ $[\text{m}^3 * \text{s}^{-1}]$ is evaluated through Eq. (1), which takes into account the population density n_{res} and n_{ind}, the occupied areas and the monthly water volume consumptions $\text{V}_{\text{monthly\_res}}$ $[\text{m}^3]$ and $\text{V}_{\text{monthly\_ind}}$ $[\text{m}^3]$ of both residential and industrial end users, respectively:

$$\bar{\dot{Q}}_{avg\_yearly} = \frac{(n_{res} \cdot A_{res} \cdot V_{monthly\_res} + n_{ind} \cdot A_{ind} \cdot V_{monthly\_ind}) \cdot \#\ of\ months\ in\ a\ year}{86{,}400 s \cdot \#\ of\ days\ in\ a\ year}\ [m^3 * s^{-1}] \qquad (1)$$

It is worth noting that Eq. (1) is valid when the flow rate coming from the water source is the same of the one that flows inside a loading/head compensation tank; indeed, the balance of the water consumption related to the end users served by a loading/head compensation tank returns the volume of the water entered the loading/head compensation tank itself. That said, Eq. (1) can be considered be a good starting point for estimating the flow rate of an ex-novo WSS.

However, when preloading tanks are located at lower geodetic heights than loading/head compensations ones, another approach for the evaluation of the flow rate is used. In this case, the monthly average flow rate pumped by the pumping station $\bar{\dot{Q}}_{\text{pump avg\_monthly}}$ $[\text{m}^3 * \text{s}^{-1}]$ is estimated by knowing its monthly electricity consumption $\overline{\text{En}}_{\text{electric,pump}}$ $[\text{MW} * \text{h}]$. The steps used in the presented methodology are explained hereinafter:

1. the number of end users served by each pump of the pumping station, as well as the monthly water volume consumption of each end user $\text{V}_{\text{monthly,end user,i}}$ $[\text{m}^3]$, are known; thus, the multiplication of the previous mentioned terms returns the water volume consumption of all the end users. Then, this value is divided by the period of operation of the WSS equal to

86,400 s times the number of days in a month, leading to the monthly average flow rate $\bar{\dot{Q}}_{pump,i\ avg\_monthly}$ $[m^3 * s^{-1}]$ elaborated by each pump;

2. both dimensions and physical characteristics of the adduction pipelines that connect each pump to the respective loading/head compensation tank are known as well. The monthly average flow rate elaborated by each pump $\bar{\dot{Q}}_{pump,i\ avg\_monthly}$ $[m^3 * s^{-1}]$ previously evaluated is used to calculate the head losses along each adduction pipeline, being a quadratic function of the flow rate;
3. the useful head H_{useful} $[m]$ provided by each pump is equal to the sum of the geodetic height difference between the head compensation tank and the preloading one $H_{available}$ $[m]$ plus the head losses along the adduction pipelines H_{loss} $[m]$ using the one-term quadratic formula valid for fully turbulent flow regimes [29];
4. since the pumps are installed in parallel, the same hydraulic efficiency within all the operating range is assumed, since they operate close to their Best Efficiency Point (BEP) most of the time. Therefore, Eq. (2) provides the monthly average electric energy $\overline{En}_{electric\_pump,i}$ $[MW * h]$ consumed by each pump:

$$\overline{En}_{electric\_pump,i} = \frac{\rho \cdot g \cdot \bar{\dot{Q}}_{pump,i\ avg\_monthly} \cdot H_{useful}}{\eta_{pump} \cdot 10^6} \cdot (24\ h \cdot \#\ of\ days\ in\ a\ month)\ [MW * h] \qquad (2)$$

5. the sum of the electric energies consumed by each pump has to be equal to the one in the electric bill; if not, the monthly water volume consumption $\bar{V}_{monthly,end\ user,i}$ $[m^3]$ of each end user is modified iteratively until the solution converges;
6. finally, when the convergence of the solution is reached, the sum of the monthly average flow rates elaborated by each pump $\bar{\dot{Q}}_{pump,i\ avg\_monthly}$ $[m^3 * s^{-1}]$ leads to the monthly average flow rate elaborated by the pumping station $\bar{\dot{Q}}_{pump\ avg\_monthly}$ $[m^3 * s^{-1}]$.

In order to have a better overview of the entire process, Figure 3 shows the flow diagram related to the procedure previously explained, where the free parameter and the known values are highlighted in dark blue and red, respectively.

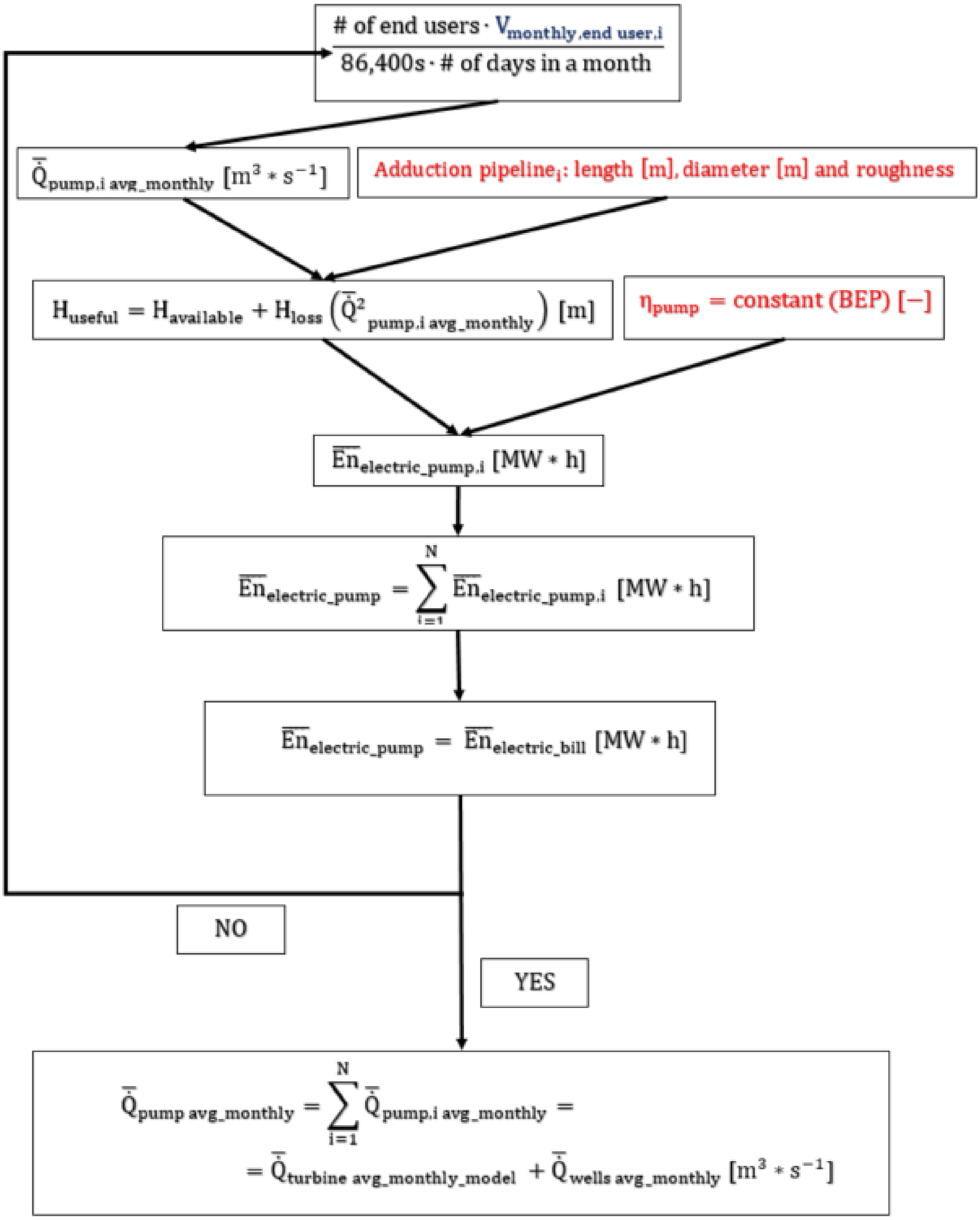

Figure 3: Flow diagram related to the estimation of the flow rate elaborated by the pumping station

As reported in Figure 3, the monthly average flow rate elaborated by the pumping station $\bar{\dot{\mathrm{Q}}}_{\mathrm{pump\ avg\_monthly}}$ $[\mathrm{m}^3 * \mathrm{s}^{-1}]$ is equal to the one elaborated by the hydraulic turbine $\bar{\dot{\mathrm{Q}}}_{\mathrm{turbine\ avg\_monthly\_model}}$ $[\mathrm{m}^3 * \mathrm{s}^{-1}]$ plus the monthly average water flow rate coming from the wells $\bar{\dot{\mathrm{Q}}}_{\mathrm{wells\ avg\_monthly}}$ $[\mathrm{m}^3 * \mathrm{s}^{-1}]$, which is obtained through flow meters installed in correspondence of the wells. Using this procedure, the water mass balance in the preloading tank is assessed; however, it is worth noting that this methodology is valid only if the variability of the flow rate in gravity adduction pipelines is restricted close to its average value.

Knowing the monthly average flow rate elaborated by the hydraulic turbine $\bar{\dot{\mathrm{Q}}}_{\mathrm{turbine\ avg\_monthly\_model}}$ $[\mathrm{m}^3 * \mathrm{s}^{-1}]$, the yearly average flow rate $\bar{\dot{\mathrm{Q}}}_{\mathrm{turbine\ avg\_yearly\_model}}$ $[\mathrm{m}^3 * \mathrm{s}^{-1}]$ is obtained through Eq. (3), where 12 stands for the number of months in a year:

$$\bar{\dot{Q}}_{turbine\ avg\_yearly\_model} = \frac{\sum_1^{12} \bar{\dot{Q}}_{turbine\ avg\_monthly\_model}}{12} \, [m^3 * s^{-1}] \tag{3}$$

Then, knowing both dimensions and physical characteristics of the gravity adduction pipeline as well, the head losses in gravity adduction pipelines are obtained according to [29]. The useful head $\mathrm{H}_{\mathrm{useful}}$ [m] that the hydraulic turbine has to exploit is equal to the difference between the available head $\mathrm{H}_{\mathrm{available}}$ [m] and the pressure losses $\mathrm{H}_{\mathrm{loss}}$ [m] that the water encounters along the gravity adduction pipeline using the one-term quadratic formula valid for fully turbulent flow regimes [29], as described by Eq. (4):

$$H_{useful} = H_{gross} - H_{loss}\left(\bar{\dot{Q}}^2{}_{turbine\ avg\_yearly\_model}\right) \ [m] \tag{4}$$

2.3 Selection of the hydraulic turbine together with power and energy calculations

The values of both flow rate $\dot{Q}$ $[\mathrm{m}^3 * \mathrm{s}^{-1}]$ and head H [m] of the hydraulic turbine, along with its angular rotational speed $\omega\,[\mathrm{rad} * s^{-1}]$ that is dependent on both grid frequency and characteristics of the electric generator, allows to select the proper machine to be installed close to the preloading tank. In particular, the most important dimensionless parameter that characterizes which machine better suits the available operative conditions is the specific speed ω_s $[-]$, as expressed by Eq. (5).

$$\omega_s = \omega \cdot \frac{\dot{Q}^{0.5}}{(gH)^{0.75}}\ [-] \tag{5}$$

However, a machine capable to operate in a quite wide range of flow rates has to be selected, preferably with a quite flat efficiency trend. Among traditional turbines, the Pelton one could be the best choice according to what previously said: indeed, the efficiency trend is quite flat close to the BEP, thus being suitable for this case study. Nevertheless, attention must be paid at strong part-load conditions, since a consistent efficiency drop occurs. This situation mainly happens in the summer season, when the water availability could be low [30]. The monthly average power that can be produced by the hydraulic turbine $\overline{\mathrm{P}}_{\mathrm{turbine\ avg\_monthly}}$ [MW] is evaluated through Eq. (6), while the potential monthly average energy recovery $\overline{\mathrm{En}}_{\mathrm{electric\_turbine\ avg\_monthly}}$ $[\mathrm{MW} * \mathrm{h}]$ is evaluated using Eq. (7), where a WSS operation of 24 h times the number days in a month has been considered. The results can be widened to a yearly basis with equations similar to Eq. (3).

$$\bar{P}_{turbine\ avg\_monthly} = \frac{\eta_{turbine} \cdot \rho \cdot g \cdot \bar{\dot{Q}}_{turbine\ avg\_monthly} \cdot H_{useful}}{10^6} = \frac{\eta_{turbine} \cdot \bar{P}_{hydraulic\ avg\_monthly}}{10^6}\ [MW] \tag{6}$$

$$\overline{En}_{electric\_turbine\ avg\_monthly} = \bar{P}_{turbine\ avg\_monthly} \cdot (24h \cdot days\ in\ a\ month)\ [MW * h] \tag{7}$$

3. CASE STUDY

3.1 Evaluation and assessment of the yearly average flow rate in gravity adduction pipelines

As already stated in Section 2, the monthly average electric energy $\overline{\mathrm{En}}_{\mathrm{electric\_turbine\ avg\_monthly}}$ $[\mathrm{MW} * \mathrm{h}]$ consumed by the pumping station, together with the useful head $\mathrm{H}_{\mathrm{useful}}$ $[\mathrm{m}]$ and their efficiencies η_{pump} $[-]$ (see Table 2), allows to estimate the monthly average flow rate elaborated by the pumping station $\overline{\dot{\mathrm{Q}}}_{\mathrm{pump\ avg\_monthly}}$ $[\mathrm{m}^3 * \mathrm{s}^{-1}]$ through Eq. (2). Furthermore, the obtained monthly average flow rate elaborated by the pumping station $\overline{\dot{\mathrm{Q}}}_{\mathrm{pump\ avg\_monthly}}$ $[\mathrm{m}^3 * \mathrm{s}^{-1}]$ has to be shortened by the the water flow rates coming from the wells $\overline{\dot{\mathrm{Q}}}_{\mathrm{wells\ avg\_yearly}}$ $[\mathrm{m}^3 * \mathrm{s}^{-1}]$. Finally, the monthly average flow rate elaborated by the hydraulic turbine $\overline{\dot{\mathrm{Q}}}_{\mathrm{turbine\ avg\_monthly\_model}}$ $[\mathrm{m}^3 * \mathrm{s}^{-1}]$ is obtained, which can be also expressed as yearly average flow rate $\overline{\dot{\mathrm{Q}}}_{\mathrm{turbine\ avg\_yearly\_model}}$ $[\mathrm{m}^3 * \mathrm{s}^{-1}]$ according to Eq. (3). Table 3 sums up the numerical values of the magnitudes previously mentioned related to the year 2018.

It is worth noting that the overall efficiency of each pump η_{pump} has been set equal to 0.65, according to the point 4 of Subsection 2.2 and the available datasheets. Furthermore, the monthly water consumption of each end user $\mathrm{V}_{\mathrm{monthly,end\ user,i}}$ $[\mathrm{m}^3]$ provided by each pump is considered the same and equal to 12 m^3, taking into account an average water volume consumption of about 0.4 m^3*day^{-1} per each end user [29]. This was possible since the distribution of the end users per each pump is homogeneous in terms of both residential and industrial consumers.

Table 2: Input and known values used in the proposed methodology

# of the PUMP	# of end users	$V_{monthly,end\ user,i}$ [m³]	Adduction pipeline length [km]	Adduction pipeline diameter [m]	$H_{available}$ [m]	η_{pump} [−]
1 (TANK A to TANK 13)	7203	12	2.94	0.25	203	0.65
2 (TANK A to TANK 22)	668	12	2.65	0.15	163	0.65
3 (TANK A TO TANK 23)	379	12	2.02	0.15	83	0.65
4 (TANK A TO TANK 24)	710	12	2.84	0.15	63	0.65

Table 3: Estimated monthly average flow rates in the analysed gravity adduction pipelines (year 2018)

MONTH (YEAR 2018)	PUMP	$En_{electric\_pump,i}$ [MW*h]	$\dot{Q}_{pump,i\ avg\_monthly\_model}$ [$m^3 s^{-1}$]	$\dot{Q}_{pump\ avg\_monthly\_model}$ [$m^3 s^{-1}$]	$\dot{Q}_{wells\ avg\_monthly}$ [$m^3 s^{-1}$]	$\dot{Q}_{turbine\ avg\_monthly\_model}$ [$m^3 s^{-1}$]
JANUARY	1	83.55	0.03543	0.04406	0.00793	0.03613
	2	6.00	0.00328			
	3	1.73	0.00186			
	4	2.51	0.00349			
FEBRUARY	1	73.86	0.03468	0.04313	0.007763	0.03537
	2	5.31	0.00321			
	3	1.53	0.00182			
	4	2.22	0.00342			
MARCH	1	94.37	0.04002	0.04977	0.02241	0.02736
	2	6.79	0.00371			
	3	1.96	0.00210			
	4	2.83	0.00394			
APRIL	1	84.27	0.03693	0.04593	0.01791	0.02802
	2	6.06	0.00342			
	3	1.75	0.00194			
	4	2.53	0.00364			
MAY	1	91.42	0.03877	0.04822	0.01917	0.02905
	2	6.57	0.00359			
	3	1.90	0.00204			
	4	2.75	0.00382			

JUNE	1	91.32	0.04002	0.04977	0.0214	0.02837
	2	6.57	0.00371			
	3	1.89	0.00210			
	4	2.74	0.00394			
JULY	1	99.67	0.04227	0.05258	0.02156	0.03102
	2	7.18	0.00392			
	3	2.07	0.00222			
	4	3.00	0.00417			
AUGUST	1	101.63	0.04310	0.0536	0.02091	0.03269
	2	7.30	0.00399			
	3	2.11	0.00226			
	4	3.05	0.00425			
SEPTEMBER	1	91.89	0.04027	0.05009	0.02254	0.02755
	2	6.61	0.00373			
	3	1.91	0.00212			
	4	2.76	0.00397			
OCTOBER	1	97.32	0.04127	0.05133	0.02258	0.02875
	2	6.99	0.00382			
	3	2.02	0.00217			
	4	2.93	0.00407			
NOVEMBER	1	91.32	0.04002	0.04977	0.0229	0.02687
	2	6.57	0.00371			
	3	1.89	0.00210			
	4	2.74	0.00394			
DECEMBER	1	97.50	0.04135	0.05143	0.02211	0.02932
	2	7.01	0.00383			
	3	2.02	0.00217			
	4	2.93	0.00408			

After the estimation of the monthly average flow rate that can be elaborated by the hydraulic turbine $\bar{\dot{Q}}_{\text{turbine avg\_monthly\_model}}$ $[m^3 * s^{-1}]$, the management of the WSS decided to install a flow meter in the gravity adduction pipeline that connects the water source to the preloading tank. The flow meter allows to evaluate the exact flow rate values that can be elaborated by the hydraulic turbine and, at the same time, to validate the estimated results obtained with the proposed methodology. Figure 4 shows the hydraulic turbine installation site highlighted in red and connected to the gravity adduction pipeline highlighted in magenta. The location of the PRV to be dismissed is also present. Table 4 lists the estimated monthly average flow rate $\bar{\dot{Q}}_{\text{turbine avg\_monthly\_model}}$ $[m^3 * s^{-1}]$ and the measured ones $\bar{\dot{Q}}_{\text{turbine avg\_monthly\_meas}}$ $[m^3 * s^{-1}]$, along with the relative percentage errors expressed by Eq. (8).

$$\Delta\bar{\dot{Q}}\ (\%) = \frac{\bar{\dot{Q}}_{turbine\ avg\_monthly\_model} - \bar{\dot{Q}}_{turbine\ avg\_monthly\_meas}}{\bar{\dot{Q}}_{turbine\ avg\_monthly\_meas}}\ [-] \quad (8)$$

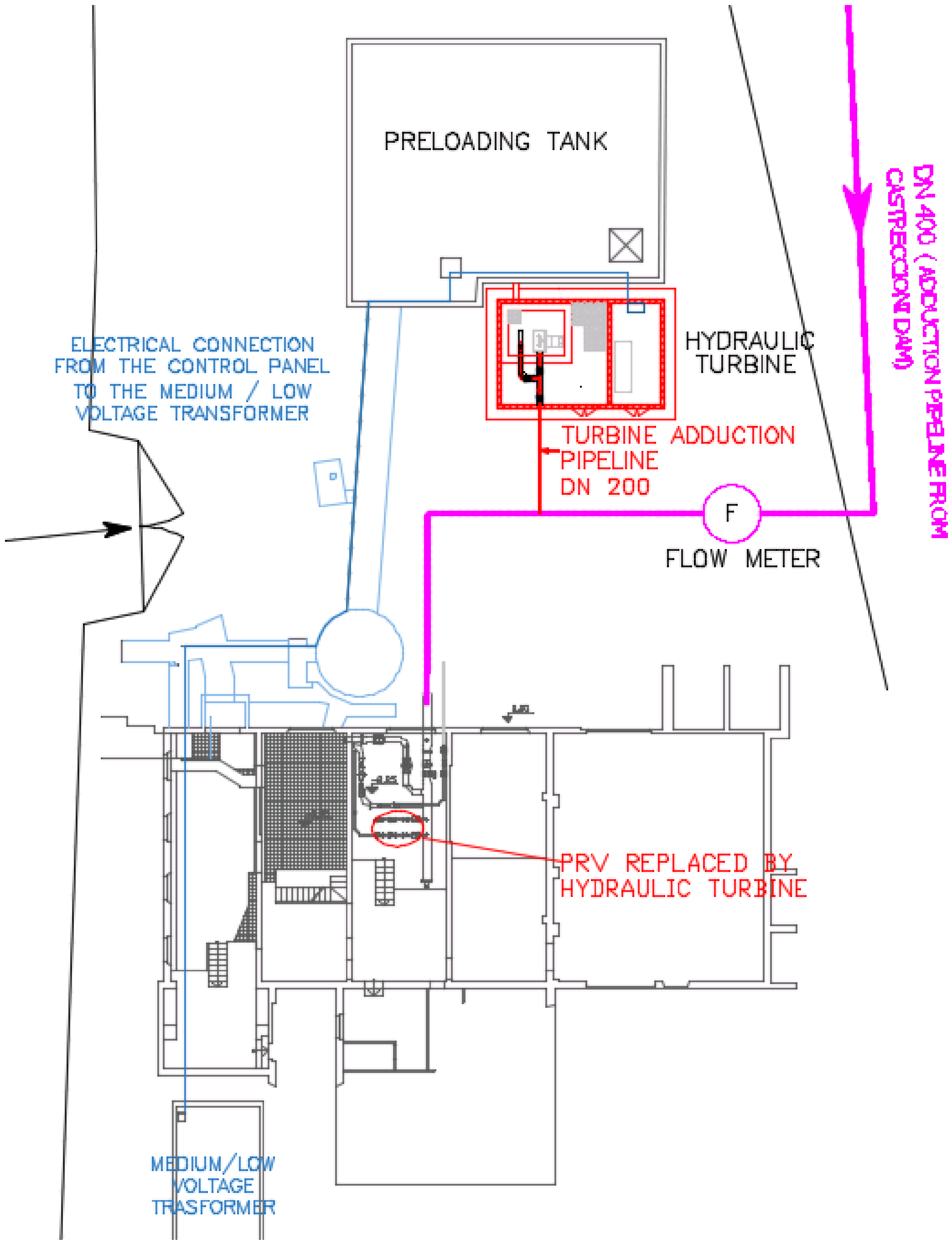

Figure 4: Detailed view of the hydraulic turbine installation site

Table 4: Monthly average flow rates elaborated by the hydraulic turbine (model. vs meas.)

MONTH (YEAR 2018)	$\dot{\mathbf{Q}}_{\text{turbine avg\_monthly\_meas}}$ $[\mathbf{m^3*s^{-1}}]$	$\dot{\mathbf{Q}}_{\text{turbine avg\_monthly\_model}}$ $[\mathbf{m^3*s^{-1}}]$	**Δ (%)**
JANUARY	0.03600	0.03613	0.36
FEBRUARY	0.02940	0.02674	-9.05
MARCH	0.02881	0.02736	-5.03
APRIL	0.02994	0.02802	-6.41
MAY	0.03074	0.02905	-5.50
JUNE	0.02983	0.02837	-4.89
JULY	0.03183	0.03102	-2.54
AUGUST	0.03497	0.03269	-6.52
SEPTEMBER	0.02628	0.02755	4.83
OCTOBER	0.02955	0.02875	-2.71
NOVEMBER	0.02935	0.02687	-8.45
DECEMBER	0.02939	0.02932	-0.24
2018	**0.03050**	**0.03000**	**-1.64**

Table 4 shows that the relative percentage errors related to the monthly average flow rates in the year 2018 are lower than 5% in six out of twelve months, while they are slightly higher (5-7%) in four out of twelve months in the same year. The remaining months present relative percentage errors between 7-10%, which are still acceptable. Nevertheless, it is pointed out that the relative percentage error referred to the yearly average flow rate potentially exploited by the hydraulic turbine $\bar{\dot{Q}}_{\text{turbine avg\_yearly\_model}}$ $[m^3 * s^{-1}]$ is sensibly lower than 5%, namely 1.64% in absolute value. It can be stated that the methodology presented in this paper is anyway a good approach for estimating the yearly average flow rate in gravity adduction pipelines when flow meters are not installed. Knowing the measured yearly average flow rate $\bar{\dot{Q}}_{\text{turbine avg\_yearly\_meas}}$ $[m^3 * s^{-1}]$, which will be renamed

$\bar{\dot{\mathrm{Q}}}_{\mathrm{turbine\ avg\_yearly}}$ $[\mathrm{m}^3 * \mathrm{s}^{-1}]$ hereinafter, the pressure losses $\mathrm{H}_{\mathrm{loss}}$ [m] between the water source and the preloading tank is calculated, being equal to 68.1 m. Therefore, the useful head that can be exploited by the hydraulic turbine $\mathrm{H}_{\mathrm{useful}}$ [m], considering the respective geodetic heights of the water source (346 m) and the preloading tank (57 m), is equal to 220.9 m. Finally, the operative yearly average measured flow rate $\bar{\dot{\mathrm{Q}}}_{\mathrm{turbine\ avg\_yearly}}$ $[\mathrm{m}^3 * \mathrm{s}^{-1}]$ of 0.0305 $\mathrm{m}^3 * \mathrm{s}^{-1}$ and the useful head exploited by the hydraulic turbine $\mathrm{H}_{\mathrm{useful}}$ [m] of 220.9 m allow to evaluate the available yearly average hydraulic power $\bar{\mathrm{P}}_{\mathrm{hydraulic\ avg\_yearly}}$ [kW], which is approximately equal to 66 kW.

3.2 Flow duration curve

In Section 2, the main operating magnitudes to evaluate the performance of the hydraulic turbine to be installed in the gravity adduction pipeline of interest have been assessed. Nevertheless, the yearly average flow rate that can be exploited by the hydraulic turbine $\bar{\dot{\mathrm{Q}}}_{\mathrm{turbine\ avg\_yearly}}$ $[\mathrm{m}^3 * \mathrm{s}^{-1}]$ must be checked through the flow duration curve, which is fundamental to obtain the flow rate value that leads to the highest energy recovery. Immediately downstream the water reservoir, a flow meter is installed. Using data measured by this flow meter between the years 2012 and 2016 (see Table 5), both yearly average water volumes and flow rates coming from the water source are determined.

Table 5: Yearly average water volumes and flow rates coming from the water reservoir (2012-2016)

YEAR	WATER VOLUMES [km^3]	YEARLY AVERAGE FLOW RATE [$\mathrm{m}^3 * \mathrm{s}^{-1}$]
2016	946.08	0.03000
2015	1151.56	0.03652
2014	923.39	0.02928
2013	898.77	0.02850
2012	911.16	0.02889
AVERAGE VALUE	966.19	0.03064

The maximum and minimum monthly average flow rates in the five years of measurements reported in Table 5 are approximately 0.047 $m^3 * s^{-1}$ and 0.019 $m^3 * s^{-1}$, respectively. However, all the flow rates recorded in the five years of measurements provided the flow duration curve reported in Figure 5.

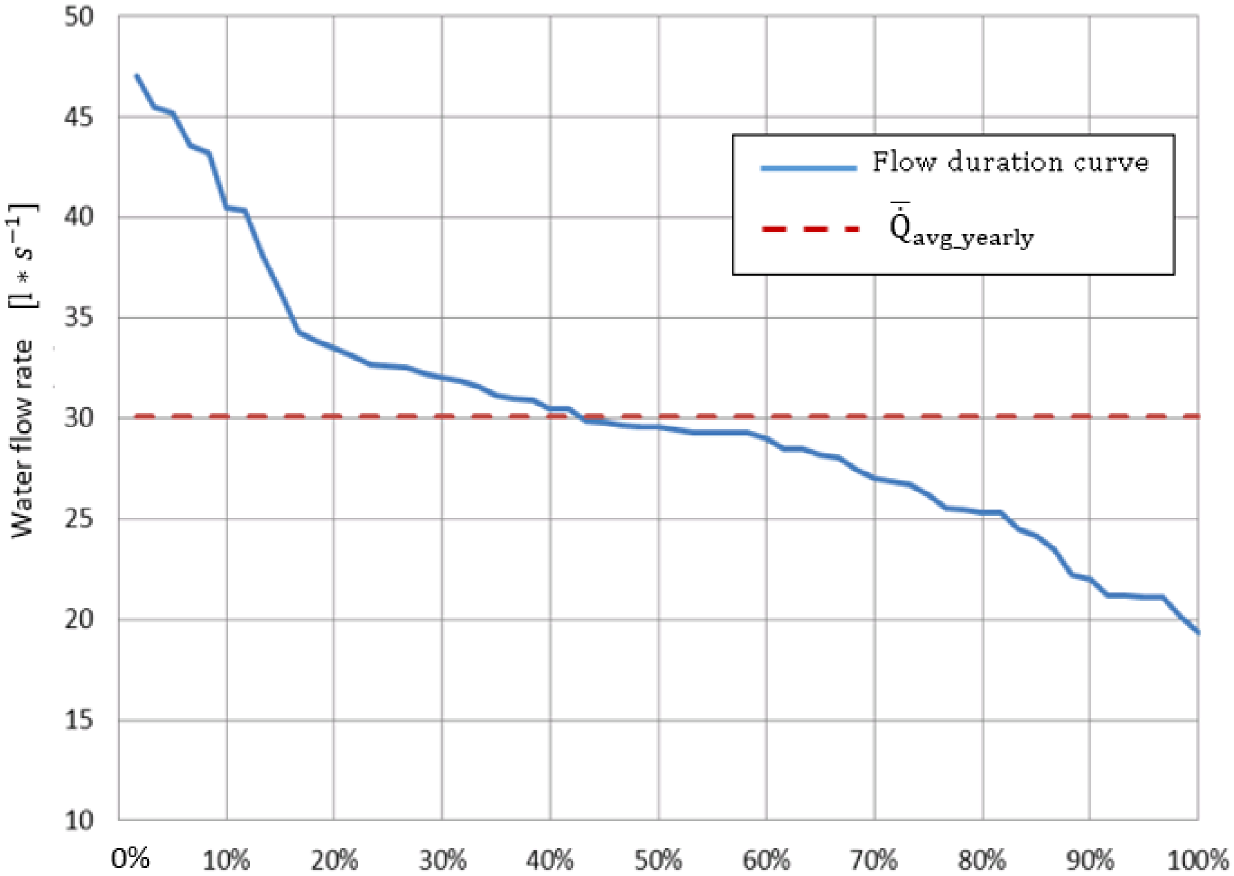

Figure 5: Flow duration curve of the gravity adduction pipeline of interest

Figure 5 clearly shows that the monthly average flow rate of about 0.03064 $m^3 * s^{-1}$ occurred more than 40% of the measured time period. That said, if a flow rate range of ±0.005 $m^3 * s^{-1}$ is considered during the operation of the hydraulic turbine, flow rates that occur up to 60% of the measured time period can be elaborated, thus further maximizing the energy recovery potential since the hydraulic turbine will be designed to have the maximum efficiency at almost 0.03064 $m^3 * s^{-1}$.

3.3 Selection of the hydraulic turbine

After the flow duration curve analysis, which confirmed the correct evaluation of the yearly average flow rate $\bar{\dot{Q}}_{turbine\ avg\_yearly}$ $[m^3 * s^{-1}]$ of 0.0305 m^3*s^{-1}, this value and the useful head H_{useful} [m] of 220.9 m, together with the rotational speed of the hydraulic turbine equal to 1000 rpm that is imposed by the electric generator, are used to evaluate the specific speed value, which is equal to 0.057, in order to select the proper hydraulic machine by means of Eq. (5). It is worth noting that this value is within the range of Pelton turbines (0.05-0.35); for this reason, this kind of hydraulic machine with two jets has been chosen for being installed in the WSS site of interest. Pelton turbines have a wide range of operation in terms of flow rates; indeed, the efficiency curve is quite flat and constant down to 30% of the maximum load and between ±40% with respect to the design flow rate [30]. For this reason, quite sensible flow rate variations from the design one do not affect too much the efficiency of this machine. The efficiency of the turbine is always constant during its operation since a Proportional-Integral-Derivative (PID) controller switch its functioning from one nozzle to two according to the operative flow rate by monitoring the water level of the preloading tank. Table 6 resumes the main characteristics of the Pelton turbine at its BEP, while Figure 6 shows the hydraulic machine installed in the site of interest.

Table 6: Pelton turbine characteristics at its BEP

MAGNITUDE	VALUE
Flow rate $[m^3*s^{-1}]$	0.0305
Useful Head [m]	220.9
Rotational speed [rpm]	1000
Total efficiency [-]	0.82
Power [kW]	54.19

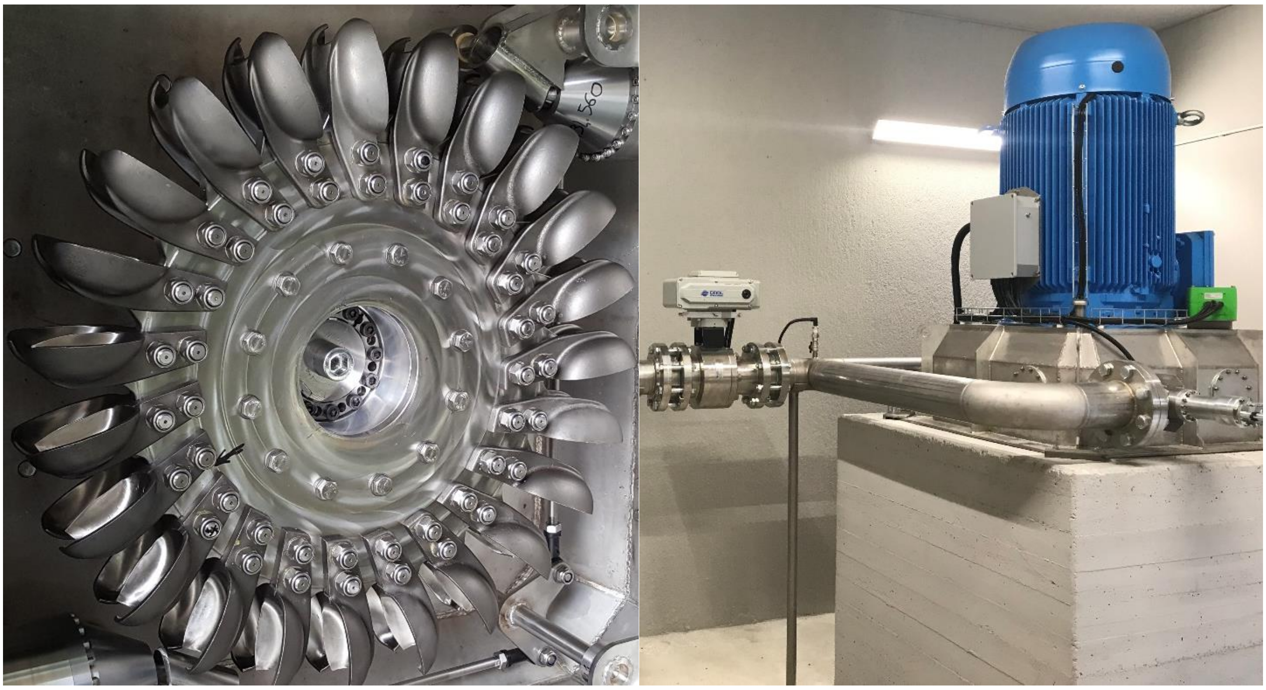

a) b)

Figure 6: Pelton turbine installed close to the preloading of the analysed WSS

4. ENERGY, ENVIRONMENTAL AND ECONOMIC ANALYSES

The values listed in Table 6 related to the Pelton turbine have been used to carry on the energy analysis deriving by the installation of a small-scale hydropower plant in WSSs. It is worth noting that the measured flow rate value at BEP has been used in these analyses.

The energy saving $\overline{\mathrm{En}}_{\mathrm{saving\_after\_turbine}}$ $[\mathrm{MW} * \mathrm{h}]$ is evaluated by the difference between the electricity consumption before, $\overline{\mathrm{En}}_{\mathrm{before\_turbine}}$ $[\mathrm{MW} * \mathrm{h}]$, and after, $\overline{\mathrm{En}}_{\mathrm{after\_turbine}}$ $[\mathrm{MW} * \mathrm{h}]$, the installation of the small-scale hydropower plant, as reported by Eq. (8).

$$\overline{En}_{saving\_after\_turbine} = \left(\overline{En}_{before\_turbine} - \overline{En}_{after\_turbine}\right) [MW * h] \tag{8}$$

Precisely, 475.25 MW*h per year are saved. To better highlight this aspect, Figure 7 shows the energy consumed by the pumping station before and after the energy recovery intervention, where the produced electric power is used for supplying electric energy to the pumping station.

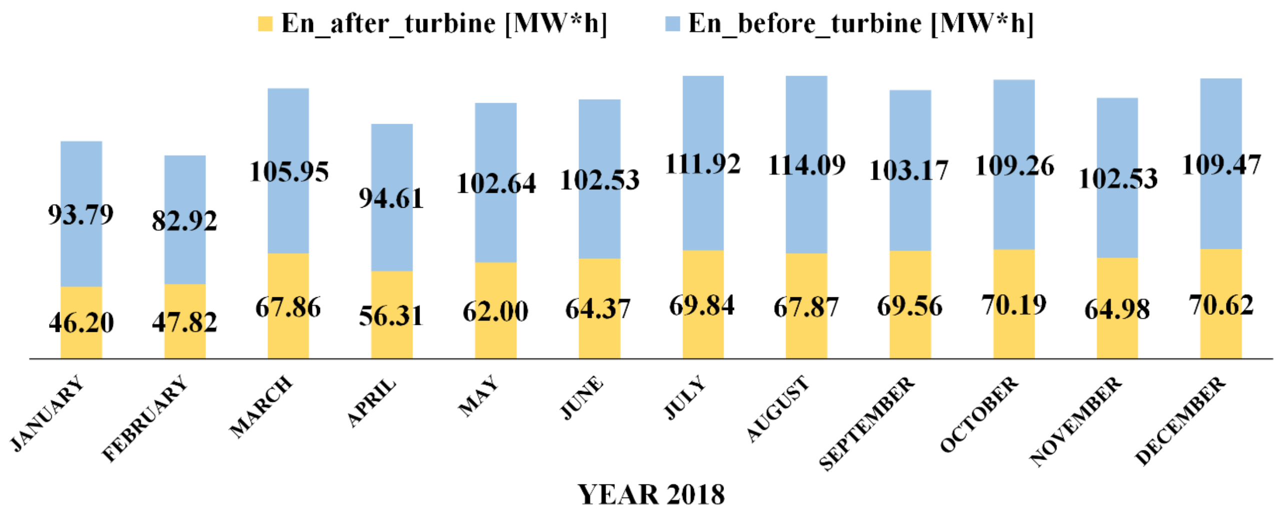

Figure 7: Electric energy consumed by the pumping station before and after the hydraulic turbine installation

It is worth noticing that the electricity consumption after the energy recovery intervention includes: i) the electricity withdrawn from the grid to feed the pumping station that is lowered due to the installation of the hydraulic turbine and ii) the electricity consumed by auxiliary devices of both pumps and turbine. Knowing the energy saving $\overline{\text{En}}_{\text{saving\_after\_turbine}}$ $[\text{MW} * \text{h}]$, 88.87 TOE are saved according to Eq. (9):

$$TOE_{saving} = \overline{En}_{saving\_after\_turbine} \cdot Fc_{TOE}\ [TOE] \qquad (9)$$

Fc_{TOE} $[\text{TEP} * (\text{kW} * \text{h})^{-1}]$ is the conversion factor equal to 0.000187 $\text{TOE} * (\text{kW} * \text{h})^{-1}$ [31] for the Italian scenario. This saving can be also expressed by means of tCO_2 not released into the atmosphere, as expressed by Eq. (10), that leads to a value of 204.36 $ktCO_2$:

$$tCO_{2\_saving} = \overline{En}_{saving\_after\_turbine} \cdot Fc_{tCO2}\ [tCO_2] \quad (10)$$

Fc_{tCO2} $[tCO_2 * (kW * h)^{-1}]$ is the conversion factor equal to $0.43\ tCO_2 * (kW * h)^{-1}$ [32]. Finally, the gross economic saving is then obtained using Eq. (11), being equal to 94.29 k€*year^{-1}:

$$Ec_{saving\_gross} = \overline{En}_{saving\_after\_turbine} \cdot F_{ec}\ [€*year^{-1}] \quad (11)$$

F_{ec} [€*year^{-1}] is the gross electricity cost in 2018 for non-residential consumers with an overall consumption of 20-500 MW*h [33]. The gross economic saving Ec_{saving_gross} $[€ * year^{-1}]$ has to be reduced by the Operation & Management (O&M) costs that have not been taken into account in this work. Nevertheless, the Italian Authorities introduced incentives for energy efficiency interventions: in this regard, energy efficiency certificates are issued according to the amount of saved TOE. In this case, the possible economic income is calculated through Eq. (12) and it is equal to 22.22 k€*year^{-1}:

$$Ec_{eec} = TOE_{saving} \cdot F_{eec}\ [€*year^{-1}] \quad (12)$$

F_{eec} [€*TOE^{-1}] corresponds to the economic income obtained per each saved TOE, considering a maximum value of 250 €*TOE^{-1} [34]. Then, Ec_{eec} [€*year^{-1}] is summed to the net economic saving Ec_{saving_gross} [€*year^{-1}], obtaining 116.51 k€*year^{-1} that is the new economic saving $Ec_{saving\_gross\_final}$ [€*year^{-1}]. This value is sensibly high and it is expected to keep such interesting results also in the upcoming years since the flow rate elaborated by the Pelton turbine is almost constant throughout the year. Table 7 resumes main energy and economic items reported in this section.

Table 7: Resume of energy, environmental and economic analyses of the energy efficiency intervention

$\overline{En}_{saving\_after\_turbine}$ $[MW * h]$	TOE_{saving}	$ktCO_{2\_saving}$	$Ec_{saving_{gross}}$ [k€*year^{-1}]	Ec_{cert} [k€*year^{-1}]	$Ec_{saving\_gross\_final}$ [k€*year^{-1}]
475.26	88.87	204.36	94.29	22.22	116.51

The management of the WSS under investigation have calculated that the construction of the civil, hydraulic, and electromechanical works to build and install the hydraulic turbine are equal to 130 k€, while the yearly operating cost is 20 k€. Thus, considering an Ec_{saving_gross} $[€ * year^{-1}]$ of 116.51 k€*year^{-1} and a discount rate of 2%, a Payback Period (PBP) of 3 years is achieved, as well as a Net Present Value (NPV) equal to 1,388,000 € in 20 years.

5. CONCLUSIONS

This paper proposes a novel methodology capable of estimating the average flow rate in a gravity adduction pipeline, upstream the preloading tank of a WSS, to evaluate a possible energy recovery intervention.

Since the installation of flow meters in gravity adduction pipelines is quite rare and the knowledge of the average flow rate is necessary to maximize the exploitation of the recoverable energy, a simple methodology for flow rate evaluation is necessary. This methodology is based on the electric energy consumption of the pumping station, since the sum of flow rates supplied by each pump is equal to the one flowing in the gravity adduction pipeline reduced by the flow rate coming from wells. It is worth noting that this methodology is valid only if the variability of the flow rate in gravity adduction pipelines is restricted close to its average value. The energy recovery intervention is evaluated for a WSS located in a mid-town in the Center of Italy. A Pelton turbine has been selected for recovering the water energy content, supplying electricity to the pumping station. The useful head exploited by the hydraulic turbine is evaluated by knowing the flow rates and the dimensions, as well as the physical characteristics, of the gravity adduction pipeline in which it can be installed.

This methodology has been then validated using flow rates values recorded by a flow meter installed in the gravity adduction pipeline after the installation of the Pelton turbine. The validation phase has shown monthly relative percentage errors lower than 5% in six out of twelve months, a slightly higher (5-7%) in four out of twelve months in the same year, and a still acceptable relative percentage error between 7-10% in the remaining months. Nevertheless, considering the yearly average flow rate value, an absolute relative percentage error of only 1.64% with respect to measured value has been obtained. Always using the measured data, an energy saving equal to 475.26 MW*h (88.87 TOE and 204.36 ktCO_2) is obtained, which results to a gross economic saving of 94.29 k€*year^{-1}. The gross economic saving increases up to 116.51 k€*year^{-1} if energy efficiency certificates issued by Italian Authorities are considered, leading to a PBP of 3 years and a NPV after twenty years of 1,388,000 €.

This study confirmed that energy recovery interventions improve the efficiency of a WSS when a proper methodology for the evaluation of the flow rates in gravity adduction pipelines is performed, which is fundamental for assessing its profitability when flow meters are not present.

In terms of future developments of this research, it would be interesting to increase the flexibility of the proposed methodology by extending the validity of the estimation of water flows, also when the flow rate to the preload tank is distributed discontinuously and not close to the yearly average one. For instance, the operation of the water pumping station could be regulated according to the average set-point level in the preloading tank by means of inverters that modulate the flow rate supplied by the pumps. Another possible development could be the evaluation of strategies that increase the self-consumption of the energy produced by the turbine (ideally up to 100%) to feed the pumping station, and modulate the pumps that feed the preload tank via inverters. Finally, another point of reflection concerns the chance of increasing the energy produced by the turbine by varying the set-point level in the preload tank and thus optimizing the regulation of the spear valve.

REFERENCES

[1] W. Hickman, A. Muzhikyan, A.M. Farid, The synergistic role of renewable energy integration into the unit commitment of the energy water nexus, Renewable Energy, Year 2017, Vol. 108, Pages 220-229.

[2] E. Ahmadi, B. McLellan, T. Tezuka, The economic synergies of modelling the renewable energy-water nexus towards sustainability, Renewable Energy, Year 2020, Vol. 162, Pages 1347-1366.

[3] J.C. Alberizzi, M. Renzi, M. Righetti, G.R. Pisaturo, M. Rossi, Speed and Pressure Controls of Pumps-as-Turbines Installed in Branch of Water-Distribution Network Subjected to Highly Variable Flow Rates, Energies, Year 2019, Vol. 12(24), Article 4738.

[4] M. Stefanizzi, T. Capurso, G. Balacco, M. Binetti, S.M. Camporeale, M. Torresi, Selection, control and techno-economic feasibility of Pumps as Turbines in Water Distribution Networks, Renewable Energy, Year 2020, Vol. 162, Pages 1292-1306.

[5] N.F. Tumen Ozdil, A. Tantekin, Exergy and exergoeconomic assessments of an electricity production system in a running wastewater treatment plant, Renewable Energy, Year 2016, Vol. 97, Pages 390-398.

[6] M. Renzi, P. Rudolf, D. Štefan, A. Nigro, M. Rossi, Installation of an axial Pump-as-Turbine (PaT) in a wastewater sewer of an oil refinery: A case study, Applied Energy, Year 2019, Vol. 250, Pages 665-676.

[7] T. Lydon, P. Coughlan, A. McNabola, Pressure management and energy recovery in water distribution networks: Development of design and selection methodologies using three pump-as-turbine case studies, Renewable Energy, Year 2017, Vol. 114, Pages 1038-1050.

[8] A. Strazzabosco, S.A. Conrad, P.A. Lant, S.J. Kenway, Expert opinion on influential factors driving renewable energy adoption in the water industry, Renewable Energy, Year 2020, Vol. 162, Pages 754-765.

[9] C.M. Papapostolou, E.M. Kondili, D.P. Zafirakis, G.T. Tzanes, Sustainable water supply systems for the islands: The integration with the energy problem, Renewable Energy, Year 2020, Vol. 146, Pages 2577-2588.

[10] X. Liu, Y. Tian, X. Lei, H. Wang, Z. Liu, J. Wang, An improved self-adaptive grey wolf optimizer for the daily optimal operation of cascade pumping stations, Applied Soft Computing, Year 2019, Vol. 75, Pages 473-493.

[11] W. Chen, T. Tao, A. Zhou, L. Zhang, L. Liao, X. Wu, K. Yan, C. Li, T.C. Zhang, Z. Li, Genetic optimization toward operation of water intake-supply pump stations system, Journal of Cleaner Production, Year 2021, Vol. 279, Article 123573.

[12] X. Zou, H. Huang, L. Li, Z. Liu, An Improved Energy-Saving Design Method for Drive System with Multi Motor-Pumps by Using Genetic Algorithm, Procedia CIRP, Year 2019, Pages 79-83.

[13] C. Zhang, L. Wang, H. Li, Optimization method based on process control of a new-type hydraulic-motor hybrid beam pumping unit, Measurement, Year 2020, Vol. 158, Article 107716.

[14] A. Mamade, D. Loureiro, D. Covas, H. Alegre, Energy Auditing As a Tool for Improving Service Efficiency of Water Supply Systems, Procedia Engineering, Vol. 89, Year 2014, Pages 557-564.

[15] C. Huang, Y. Li, X. Li, H. Wang, J. Yan, X. Wang, J. Wu, F. Li, Understanding the water-energy nexus in urban water supply systems with cities features, Energy Procedia, Vol. 152, Year 2018, Pages 265-270.

[16] M.R. Nogueira Vilanova, J.A. Perrella Balestieri, Energy and hydraulic efficiency in conventional water supply systems, Renewable and Sustainable Energy Reviews, Year 2014, Vol. 30, Pages 701-714.

[17] G. Meirelles Lima, B. Melo Brentan, E. Luvizotto, Optimal design of water supply networks using an energy recovery approach, Renewable Energy, Year 2018, Vol. 117, Pages 404-413.

[18] S. Kucukali, Hydropower potential of municipal water supply dams in Turkey: a case of study in Ulutan Dam, Energy Policy, Year 2010, Vol. 38, Pages 6534-6539.

[19] A. McNabola, P. Coughlan, A.P. Williams, Energy recovery in the water industry: an assessment of the potential of micro-hydropower, Water Environmental Journal, Year 2013, Vol. 27, Pages 1-11.

[20] J. Saldarriaga, C.A. Salcedo, Determination of Optimal Location and Settings of Pressure Reducing Valves in Water Distribution Networks for Minimizing Water Losses, Procedia Engineering, Year 2015, Vol. 119, Pages 973-983.

[21] F. García-Ávila, A. Avilés-Añazco, J. Ordoñez-Jara, C. Guanuchi-Quezada, L. Flores del Pino, L. Ramos-Fernández, Pressure management for leakage reduction using pressure reducing valves. Case study in an Andean city, Alexandria Engineering Journal, Year 2019, Vol. 58, Pages 1313-1326.

[22] C. Van den Berg, The Drivers of Non-Revenue Water: How Effective Are Non-Revenue Water Reduction Programs?, Policy Research Working Paper, 6997, Year 2014. Available at: http://documents1.worldbank.org/curated/en/949281468161359020/pdf/WPS6997.pdf (last accessed on the 05/07/2021).

[23] F. Vieira, H.M. Ramos, Hybrid solution and pump-storage optimization in water supply system efficiency: a case of study, Energy Policy, Year 2008, Vol. 36, Pages 4142-4148.

[24] Z. Xu, L. Yao, X. Chen, Urban water supply system optimization and planning: Bi-objective optimization and system dynamics methods, Computers & Industrial Engineering, Year 2020, Vol. 142, Article 106373.

[25] S. Kucukali, Municipal water supply dams as a source of small hydropower in Turkey, Renewable Energy, Vol. 35, Year 2010, Pages 2001-2007.

[26] L-T. Wong, K-W Mui, A Review of Demand Models for Water Systems in Buildings including a Bayesian Approach, Water, Volume 10(8), Year 2018, Article 1078.

[27] L.K. Letting, Y. Hamam, A.M. Abu-Mahfouz, Estimation of Water Demand in Water Distribution Systems Using Particle Swarm Optimization, Water, Volume 9(8), Year 2017, Article 593.

[28] G. Balacco, A. Carbonara, A. Gioia, V. Iacobellis, A.F. Piccinini, Evaluation of Peak Water Demand Factors in Puglia (Southern Italy), Water, Volume 9(2), Year 2017, Article 96.

[29] V. Milano, Acquedotti Guida alla progettazione (in Italian), HOEPLI, Year 2012, Pages 650.

[30] H. Jeon, J. Hoon Park, Y. Shin, M. Choi, Friction loss and energy recovery of a Pelton turbine for different spear positions, Renewable Energy, Year 2018, Vol. 123, Pages 273-280.

[31] Autorità Regolazione Energia Reti e Ambiente (ARERA), Deliberazione dell'Autorità 618/2013/R/EFR (in Italian). Available at: https://www.arera.it/allegati/docs/13/618-13.pdf (last accessed on the 05/07/2021).

[32] Agenzia nazionale per le nuove tecnologie, l'energia e lo sviluppo economico sostenibile (ENEA), Rapporto Energia e Ambiente 2002 (in Italian). Available at: http://old.enea.it/com/web/pubblicazioni/REA_02/analisi_02.pdf (last accessed on the 05/07/2021).

[33] European Statistical Office (EUROSTAT). Available at: https://ec.europa.eu/eurostat/web/energy/data/database (last accessed on the 05/07/2021).

[34] Gestore dei Servizi Energetici (GSE), Certificati bianchi (in Italian). Available at: https://www.gse.it/servizi-per-te/efficienza-energetica/certificati-bianchi (last accessed on the 05/07/2021).